International Conference on Applied Energy 2021
Nov. 29 - Dec. 2, 2021, in Bangkok, Thailand
Paper ID: 0827

Numerical Study of Combustion Modes in a Clustered Porous Radiant Burner

Sunita Deb[1*], SHV Satish [2], P Muthukumar[2]

1 School of Energy Science and Engineering, Indian Institute of Technology Guwahati, email id: sunitadeb@iitg.ac.in

2 Department of Mechanical Engineering, Indian Institute of Technology Guwahati

ABSTRACT

The combustion characteristics of a newly developed Clustered Porous Radiant Burner was investigated. Numerical simulations were performed at different equivalence ratios for a power input of 12.56 kW and the flame movement was analyzed by locating the maximum temperature points. Thermal non-equilibrium model was considered for the energy equations and the combustion was modelled by employing eddy-dissipation model. Surface combustion was reported for equivalence ratio 0.6, while the submerged combustion was obtained for equivalence ratios 0.7 to 0.85. Stable partially submerged combustion was obtained for equivalence ratio of 0.9. The burner was observed to be unstable when operated at an equivalence ratio of above 0.95. Numerically predicted result was in good agreement with the experimental data.

Keywords: Flame stability; porous radiant burner; eddy dissipation model; flashback; Rosseland model

NONMENCLATURE

Abbreviations	
CPRB	Clustered Porous Radiant Burner
CZ	Combustion Zone
PZ	Preheating Zone
PRB	Porous Radiant Burner
PMC	Porous Media Combustion
PM	Porous Matrix
Symbols	
T	Temperature
h_v	Volumetric heat transfer coefficient
k	Thermal conductivity
W	Molecular mass
w	Molar rate of species production

1. INTRODUCTION

The provision of clean and affordable cooking energy is one of the important targets of the 17 Sustainable Development Goals (SDG) pursued by the United Nations [1]. Advancing towards this goal, technological improvements are being carried out on developing less polluting and energy efficient cookstoves. In this regard, the use of Porous Media Combustion (PMC) in cookstoves has been reported to be useful in terms of fuel savings and cleaner combustion. The specialty of PMC technology lies in the heat transfer characteristics that occur due to the enthalpy exchange between the solid and the gas inside the Porous Matrix (PM). Over the last few decades, many researchers investigated various domains of PMC in order to study the thermal performance and combustion characteristics, both experimentally and numerically.

In one of the studies, Mujeebu et al. [2] highlighted that the operation of a Porous Radiant Burner (PRB) on surface combustion mode increased the thermal efficiency compared to submerged combustion mode. Janvekar et al. [3] investigated submerged and surface flames in a PRB with varied preheater thickness. In a Porous Free Flame Burner (PFFB) developed by Ghorashi et al. [4], lower axial temperature was obtained from PFFB and was stabilized at higher equivalence ratio (φ) as compared to a PRB.

In recent studies [5,6], the authors research team has demonstrated that the use of a Clustered Porous Radiant Burner (CPRB) is advantageous in increasing the thermal efficiency and reducing emissions compared to a single-PRB. These investigations were carried out for burner operation on submerged combustion mode. The novel nature of the research demands deeper investigation on the flame stability, which can contribute substantially to the design of clean and energy-efficient

Selection and peer-review under responsibility of the scientific committee of the 13th Int. Conf. on Applied Energy (ICAE2021).

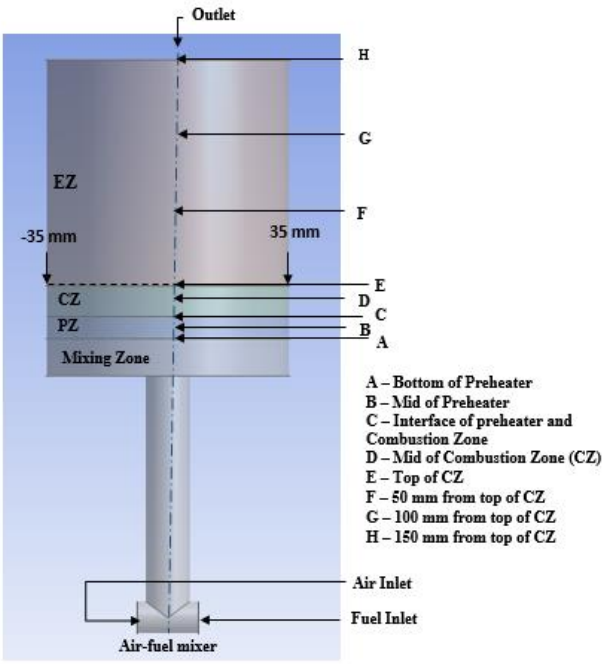

Fig. 1. Computational domain and positions for temperature measurement

burners for industrial and household applications. Previous studies exhibited the burner performance on single operating modes. The present study demonstrates for the first time a study on various combustion modes of the CPRB through numerical simulations in order to ascertain the stable operating limits of the burner.

2. METHODOLOGY

2.1 Physical Domain

Three individual PRBs of diameter 70 mm are clustered to form a CPRB. The detailed description of the set-up can be found in [6]. The individual PRBs of the CPRB are reported to function similarly and thus the temperature plots of only one individual burner is considered to be sufficient to depict the variations of temperature with φ and power input. Similarly, in this study, numerical simulations are performed on one individual burner of the CPRB. The computational domain considered in the present study represents one individual burner shown in Fig. 1. The individual burners of the CPRB are supplied with required quantities of air and fuel mixture as per the power input and φ. The φ is calculated as per the following formula [6] –

$$\varphi = 15.45 \times A/F \qquad (1)$$

where, A and F are the actual mass flow rates of air and fuel, respectively. The fuel and air enter the mixer separately through different streams and are mixed as they flow towards the burner outlet. The mixer, mixing tube and mixing space constitute the Mixing Zone (MZ). The MZ is followed by two PMs having different thermo-physical properties. The upstream porous layer serves as the Preheating Zone (PZ) and is made of Alumina (7% porosity, height: 10 mm, diameter: 70 mm), while, the downstream layer functions as the Combustion Zone (CZ) and is made of reticulated foam of Silicon Carbide (porosity 90%, height 20 mm and diameter: 70 mm). The computational domain also consists of an extended flame zone (EZ) at the top of the CZ to capture the flame movement downstream of the CZ. The axial and the radial temperature distributions are obtained at the top surface of the CZ and are plotted at locations as shown in Fig. 1.

The simulations are carried out for a steady flow process and to simplify the model, the buoyancy effects, the thickness of the materials and the walls are neglected. The reactants and products are considered to be incompressible ideal gases and the thermal properties like specific heat capacity, density and thermal conductivity re assumed to be constants.

2.2 Governing Equations

Continuity Equation –

The conservation of mass can be represented by the continuity equation as the following –

$$\nabla.\left(\rho_g \vec{u}\phi\right) = 0 \qquad (2)$$

The conservation of momentum can be represented by the momentum equation as expressed in Eq. 3 (a) and (b).

Momentum Equation –

a) For the mixing zone:

$$\nabla.\left(\rho_g \vec{u}\vec{u}\phi\right) = -\nabla p + \nabla.\left(\mu \nabla \vec{u}\right) \qquad (3a)$$

b) For the porous domains:

$$\nabla.\left(\rho_g \vec{u}\vec{u}\phi\right) = -\nabla p + \nabla.\left(\mu \nabla \vec{u}\right) - \frac{\mu}{K_1}\bar{u} - C_2 \frac{1}{2}\rho_g |\vec{u}|\vec{u} \qquad (3b)$$

where, the K_1 and C_2 represent the permeability and inertial resistance factor, respectively [6].

Species Conservation Equation –

$$\nabla.\left(\rho_g \vec{u} Y_i\right) = -\nabla.\left(\rho_g\left(D_{m,i} + D_m^d\right)\right) + w_i W_i \qquad (4)$$

Energy Equation –

Eqs. 5 (a) and (b) represent the energy conservation equations for the gas and the solid phases, respectively.

As the gas phase radiation is neglected, the radiative heat transfer term, modelled by Rosseland approximation, is incorporated in the solid phase energy equation.

a) For the gas phase:

$$\nabla\left(c_g\rho_g T_g\vec{u}\right) = \phi\nabla\left(k_g + c_g\rho_g D^t\right)\nabla T_g - \phi\sum_i w_i h_i W_i - h_v\left(T_g - T_s\right) \quad (5a)$$

b) For the solid phase:

$$\nabla(k_s + \frac{16\sigma T_s^3}{3\alpha})\nabla T_s - h_v\left(T_s - T_g\right) = 0 \quad (5b)$$

In the above equations, ϕ, $\vec{u}$, p, μ and ρ_g represent the porosity, velocity vector, pressure, viscosity and density of gas, respectively. In Eqs. (4) – (5b), $D_{m,i}$, D_m^d and D^t represent the diffusivity, dispersion of species "i" and the thermal dispersion, respectively. The gas and the solid phases are denoted by the subscripts g and s, respectively. The notations α and σ represent the absorption coefficient and the Stefan-Boltzmann constant, respectively. The combustion of LPG was simplified to a two-step mechanism that involved the formation of CO as intermediate and the rate of reaction was calculated by the eddy-dissipation model.

2.3 Boundary Conditions

The CPRB was operated at a fuel flow rate of 1 kg/h, which amounts to a power input of 12.56 kW [5]. As the CPRB is a cluster of three burners, the individual burners of the CPRB operate at a power input of 4.18 kW corresponding to fuel mass flow rate of 0.091 g/s. The amount of combustion air supplied is varied as per the different φ considered for the present study. The mass flow inlet boundary condition is applied both at the fuel and the air inlet. At the fuel inlet, the mole fractions of butane and propane are taken as 0.6 and 0.4, respectively, while at the air inlet, the mole fractions of oxygen and nitrogen are taken as 0.21 and 0.79, respectively. The pressure outlet boundary condition is applied at the outlet while, at the PZ and CZ walls, mixed heat transfer boundary condition comprising radiative and convective heat transfer is applied.

3. RESULTS AND DISCUSSION

3.1 Validation of the model

Initially, a grid independence test is conducted to find the optimum mesh for the simulations at φ of 0.8. The temperature at position 'E' obtained from the optimized mesh is then compared with that of experimental results of [5] to establish the accuracy of the model and validate the same. The results of the grid independence test and the subsequent comparison with experimental results are presented in Table 1.

Table 1: Grid impendence test and model validation with experimental data.

Mesh elements	Temperature at position 'E' (°C)
658128	1120
723941	**1082**
796335	1084
Experimental	**1063 [5]**

The mesh with 723941 elements is chosen to be the optimum mesh for the simulations because a further reduction in mesh size does not improve the results. As the deviation from the experimental results is less than 5%, the numerical model adopted is deemed to be appropriate for the numerical study.

3.2 Investigation on the surface and submerged combustion modes

The plots of variation of axial temperature along the positions shown in Fig. 1, are presented in Fig. 2. The maximum axial temperature representing the flame temperature is observed to increase with φ. With the increase in φ from 0.6 to 0.7, the flame is observed to shift upstream. In case of φ values of 0.7 and 0.75, the maximum temperature is found at the interface of the CZ and the PZ. On the other hand, in case of burner operation at φ values of 0.8, 0.85 and 0.9, the maximum temperature is obtained at a position 3 mm upstream of the CZ and PZ interface. In case of φ of 0.9, although the maximum temperature is obtained below the PM interface, the flame extended beyond the CZ, denoting partially-submerged combustion, as indicated by temperatures more than 1200°C. In case of φ of 0.95, the flame, however, shifted downstream and the maximum temperature obtained is 1412°C. Nevertheless, the combustion can be regarded as unstable as the temperature at the bottom of the mixing zone reached 200°C, resulting from the recirculated heat from upstream of the PZ. Such high temperature in the upstream section of the burner can lead to flashback hampering safe operation.

For φ values of 0.6 and 0.65, the maximum flame temperatures are 909°C and 1128°C, respectively, which

are obtained at 2 mm downstream of the CZ and at the mid of the CZ, respectively, indicating surface and partially submerged combustion, respectively.

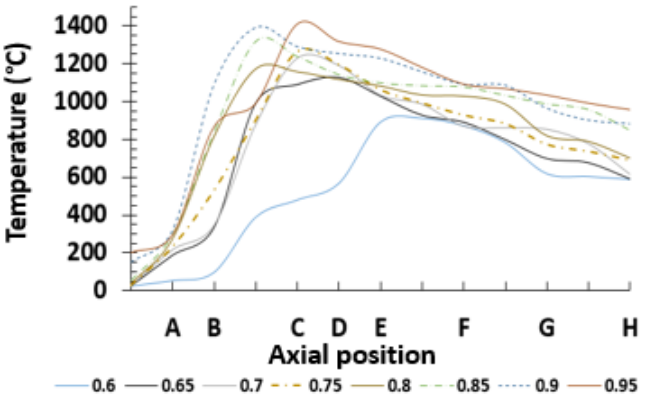

Fig. 2. Variation of axial temperature with equivalence ratio

Stable submerged combustion is observed to occur for φ values of 0.7 to 0.85, which is validated from the results obtained by Deb and Muthukumar [5].

3.2 Variation of top surface temperature

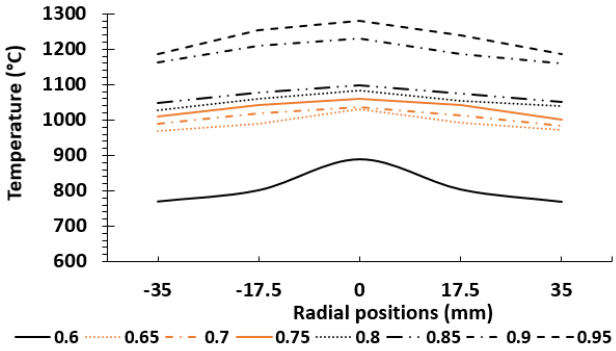

Fig. 3. Variation of radial temperature with equivalence ratio

The variation of the top surface temperature with φ is shown in Fig. 3. A striking difference among the temperature distributions is observed when the burner is operated at the stable and the limiting values of φ. At φ of 0.6 and 0.95, the difference between the temperatures at the centre and the peripheral positions is found to be more than 90°C, while in case of the stable range of φ, the difference is limited to 50°C. The above findings infer that the stable burner operation in the stable φ range also yielded more uniform heat output across the burner surface.

4. Conclusion

A numerical study on the influence of equivalence ratio (φ) on the mode of combustion and safe operation has been conducted for a Clustered Porous Radiant Burner (CPRB) for a power input of 12.56 kW. Simulations were performed for forced-draft operation and the maximum values of flame temperatures were estimated. Surface combustion is found to occur at φ of 0.6. Unstable combustion is observed to take place for φ of above 0.9. Stable submerged combustion is obtained for φ of 0.7 to 0.85, while for φ of 0.65 and 0.9, partially-submerged combustion is obtained. Additionally, uniform distribution of heat across the top surface of the burner is attained for the stable φ range. The research work is extended to investigate a self-aspirated double-layered PRB to study the air entrainment and its influence on the combustion and flame stability but has not been presented to maintain the conciseness of the paper.

ACKNOWLEDGEMENT

The authors are thankful to the Ministry of Education for funding the research work through Project No: IMPRINT 6727.

REFERENCE

[1] Goal 7 | Department of Economic and Social Affairs n.d. https://sdgs.un.org/goals/goal7 (accessed September 22, 2021).

[2] Mujeebu MA, Abdullah MZ, Mohamad AA. Development of energy efficient porous medium burners on surface and submerged combustion modes. Energy 2011;36:5132–9. https://doi.org/10.1016/j.energy.2011.06.014.

[3] Janvekar AA, Miskam MA, Abas A, Ahmad ZA, Juntakan T, Abdullah MZ. Effects of the preheat layer thickness on surface/submerged flame during porous media combustion of micro burner. Energy 2017;122:103–10. https://doi.org/10.1016/j.energy.2017.01.056.

[4] Ghorashi SA, Hashemi SA, Mollamahdi M, Ghanbari M, Mahmoudi Y. Experimental investigation on flame characteristics in a porous-free flame burner. Heat Mass Transf 2020;56:2057–64. https://doi.org/10.1007/s00231-020-02840-x.

[5] Deb S, Muthukumar P. Development and performance assessment of LPG operated cluster Porous Radiant Burner for commercial cooking and industrial applications. Energy 2021;219:119581. https://doi.org/10.1016/j.energy.2020.119581.

[6] Deb S, Kaushik LK, Kumar MA, Satish SH V, Muthukumar P. Clustered Porous Radiant Burner : A cleaner alternative for cooking systems in small and medium scale applications. J Clean Prod 2021;308:127276. https://doi.org/10.1016/j.jclepro.2021.127276.